High harmonic generation with nearly circular polarized pulses

Jonathan Dubois, C. Chandre, T. Uzer

High harmonic generation with nearly circular polarized pulses

J. Dubois,[1] C. Chandre,[1] and T. Uzer[2]

[1] *Aix Marseille Univ, CNRS, Centrale Marseille, I2M, Marseille, France*
[2] *School of Physics, Georgia Institute of Technology, Atlanta, Georgia 30332-0430, USA*

According to conventional wisdom, increasing ellipticity reduces high harmonic generation by several orders because the recollision probability decreases. This is the obvious conclusion drawn from the motion of an electron in a laser field without an envelope. In contrast, we report on a recollision channel with large return energy and a substantial probability, regardless the ellipticity, in which the laser envelope plays a dominant role in the energy gained by the electron, and in the conditions for the electron to come back to the core.

High harmonic generation (HHG) in atomic or molecular gases subjected to intense infra-red laser fields heralded a new era in science and technology due to its ability to unravel the electron dynamics on its own spatial and temporal scales [1–3] and its role in realizing table-top ultrashort light sources [4–6]. Controlling HHG from the parameters of the driving laser represents a formidable challenge both on the experimental [7] and theoretical [8] sides, with considerable amount of research efforts for the past decades. For instance, changing the ellipticity of the driving laser, which acts as a simple control knob, highlights very different phenomena originating from electron dynamics [9].

The physics of HHG is built on the so-called recollisions [10, 11]. The conventional semiclassical scenario [10–12] is split in three distinct steps: (i) The electron tunnel-ionizes through the potential barrier induced by the laser field, (ii) travels in the laser field, and (iii) recombines with the portion of the wavepacket that remained bounded. This recollision picture is understood in absence of a pulse envelope. For an elliptically polarized (EP) laser field $\mathbf{E}(t) = E_0[\hat{\mathbf{x}}\cos(\omega t) + \xi\hat{\mathbf{y}}\sin(\omega t)]$, given an ionization time t_i, the position of the electron after ionization in the strong field approximation (SFA) is given by

$$\mathbf{r}(t) = \mathbf{r}(t_i) + [\mathbf{p}(t_i) - \mathbf{A}(t_i)]\,(t - t_0) + [\mathbf{E}(t) - \mathbf{E}(t_i)]/\omega^2. \tag{1}$$

The amplitude of the laser is E_0, its ellipticity is ξ and its frequency is ω. The position and the momentum of the electron are $\mathbf{r}$ and $\mathbf{p}$, respectively. The vector potential is $\mathbf{A}(t)$ such that $\mathbf{E}(t) = -\partial\mathbf{A}(t)/\partial t$. At ionization, the electron exits the potential barrier with $\mathbf{p}(t_i) = \mathbf{0}$. For $\xi = 0$, the electron leaves the ionic core with a drift momentum $-\mathbf{A}(t_i) = \hat{\mathbf{x}}(E_0/\omega)\sin(\omega t_i)$, and returns close to the core at time t_r, i.e., $\mathbf{r}(t_r) \approx \mathbf{r}(t_i)$, due to the laser oscillations $\mathbf{E}(t)/\omega^2$. For $\xi > 0$, strictly speaking the electron never comes back to the core, i.e., there is no times t_i and t_r such that $\mathbf{r}(t_r) = \mathbf{r}(t_i)$ in Eq. (1) because of the non vanishing drift momentum $-\mathbf{A}(t_i)$ in the direction transverse to the electric field, which pushes the electron away from the core [10]. In this framework, the electron can only recollide when the laser field is linearly polarized (LP).

The recollision picture can, however, be extended to near LP-fields by taking into account that after ionization, the electron is near the potential barrier. The initial momentum along the transverse direction to the laser field $p_\perp$ is distributed [13, 14] as $\propto \exp(-p_\perp^2\sqrt{2I_p}/E_0)$, with I_p the ionization potential of the recolliding electron. The initial transverse momentum compensates the initial drift momentum of the electron after ionization and recollisions become possible [15, 16]. At the threshold ellipticity $\xi_{\rm th} \approx \omega I_p^{-1/4}/\sqrt{E_0}$ (see Ref. [15], which is $\xi_{\rm th} \approx 0.2$ for the parameters we use here with $I_p = 5.7$ eV), the HHG intensity drops by a factor 10 compared to its value for $\xi = 0$. For ellipticities $\xi > \xi_{\rm th}$, the initial momentum $p_\perp \approx \xi E_0/\omega$ necessary to compensate the drift momentum is poorly weighted and the probability that the electron returns to the core drops off. Moreover, if the electron returns to the core, we find that the energy it gains during the recollision is

$$\Delta\mathcal{E} = \kappa \mathrm{U}_p(1 - \xi^2), \tag{2}$$

with $\mathrm{U}_p = E_0^2/4\omega^2$ the ponderomotive energy and $0 \leq \kappa \lesssim 3.17$. Hence, the recolliding electrons, if any, do not bring back enough energy from the laser field at high ellipticities to trigger high harmonic radiation. Consequently, the three-step model predicts that the high frequency part of the HHG spectra is suppressed with elliptically polarized lights.

All the analysis above is done in absence of pulse envelope. We find that the presence of an envelope drastically affects these conclusions. In this Letter, we identify a highly probable recollision channel with large return energy by accounting for the effects of the pulse envelope $f(t)$, which is particularly effective for nearly circular polarizations. We show that it is the competition between the Coulomb force and the laser field that makes this recollision channel highly probable by creating a channel of ionization early after the laser field is turned on. After ionization, the amplitude of the vector potential is small, and therefore the sideways drift of the electron can be compensated by its momentum after ionization. Furthermore, we show that this recollision channel and the return of the electron can be understood using the SFA, in opposition with the conventional three-step model for which the laser envelope is constant.

We first demonstrate the existence of this recollision channel for the least favorable case in the conventional recollision scenario, namely the circularly polarized (CP)

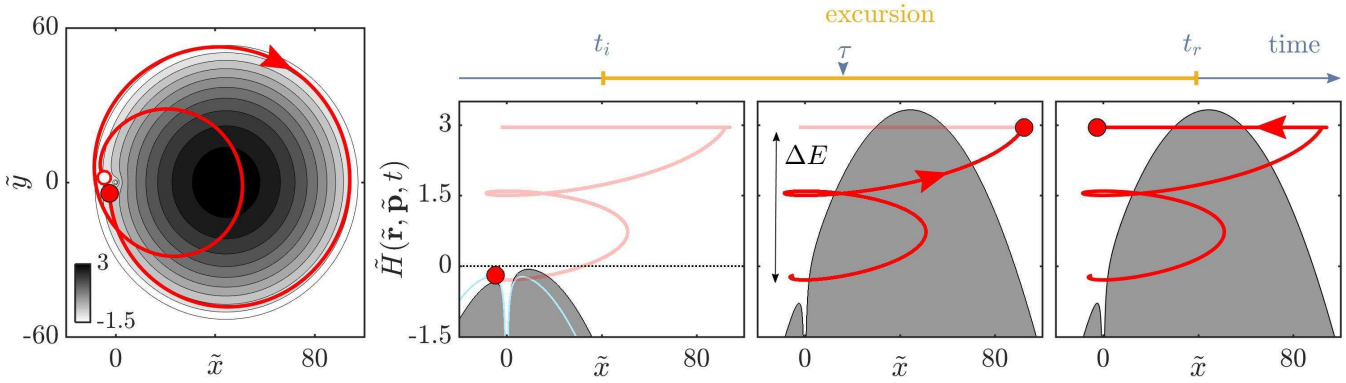

FIG. 1: Typical recollision with a high return energy: From the ground state to the return for a 2-4-2 laser envelope. Left panel: Trajectory in the rotating frame $(\tilde{x},\tilde{y})$. The white and red circles are the position of the electron at the ionization and recombination time, respectively. The color shows the value of the zero-velocity surface during the plateau. Right panels: The trajectory projected along the position and energy of Hamiltonian (3) at time $t_i \approx 0.3T$, $\tau = 2T$ and $t_r \approx 2.6T$ (from left to right). The grey surface is the classical forbidden region for $\tilde{y} = 0$ $[\tilde{H}(\tilde{\mathbf{r}},\tilde{\mathbf{p}},t) < \mathcal{Z}(\tilde{\mathbf{r}},t)]$. The light blue curve is the zero-velocity surface at time $t = 0$ for $y = 0$. The saddle point is the local maximum of the zero-velocity surface for negative $\tilde{x}$. Distances and energies are in a.u.

case ($\xi = 1$). We describe the electron dynamics in a rotating frame (RF) of basis vectors $(\hat{\mathbf{x}},\hat{\mathbf{y}},\hat{\mathbf{z}})$. In the RF, the CP field is unidirectional, the position and the momentum of the electron are $\tilde{\mathbf{r}} = \mathbf{R}(t)\mathbf{r}$ and $\tilde{\mathbf{p}} = \mathbf{R}(t)\mathbf{p}$, with $\mathbf{R}(t)$ the rotation matrix of angle ωt. The classical single-active electron Hamiltonian, in the dipole approximation, reads

$$H(\tilde{\mathbf{r}},\tilde{\mathbf{p}},t) = \frac{|\tilde{\mathbf{p}}|^2}{2} - \omega\tilde{\mathbf{p}}\cdot\hat{\mathbf{z}}\times\tilde{\mathbf{r}} + V(\tilde{\mathbf{r}}) + \tilde{x}E_0 f(t), \quad (3)$$

where the term $-\omega\tilde{\mathbf{p}}\cdot\hat{\mathbf{z}}\times\tilde{\mathbf{r}}$ is the Coriolis potential. Atomic units are used unless stated otherwise. We use a laser wavelength of 780 nm (corresponding to $\omega = 0.0584$ a.u.), a laser intensity of 8×10^{14} W $\cdot$ cm^{-2} (corresponding to $E_0 = 0.151$ a.u.), and the soft Coulomb potential [17] $V(\mathbf{r}) = -(|\mathbf{r}|^2 + a^2)^{-1/2}$ with $a = 0.262$. At each time, the energy of the system is above the so-called zero-velocity surface $H(\tilde{\mathbf{r}},\tilde{\mathbf{p}},t) \geq \mathcal{Z}(\tilde{\mathbf{r}},t)$, with $\mathcal{Z}(\tilde{\mathbf{r}},t) = -\omega^2|\tilde{\mathbf{r}}|^2/2 + V(\tilde{\mathbf{r}}) + \tilde{x}E_0 f(t)$. The surface where $H(\tilde{\mathbf{r}},\tilde{\mathbf{p}},t) = \mathcal{Z}(\tilde{\mathbf{r}},t)$ is depicted in the left panel of Fig. 1 and is called the zero-velocity surface, i.e., the surface in phase space such that $\mathrm{d}\tilde{\mathbf{r}}/\mathrm{d}t = \mathbf{0}$ and corresponds to the condition $\tilde{\mathbf{p}} = \omega\hat{\mathbf{z}}\times\tilde{\mathbf{r}}$. In the adiabatic approximation, there exists three fixed points of the dynamics: At the top of the zero-velocity surface and mainly due to the laser interaction $[\tilde{\mathbf{r}} \approx \hat{\mathbf{x}}f(t)E_0/\omega^2]$, around the origin and mainly due to the soft Coulomb potential ($\tilde{\mathbf{r}} \approx \mathbf{0}$), and at the saddle point $\tilde{\mathbf{r}}^\star = \hat{\mathbf{x}}\tilde{x}^\star$ with $\tilde{x}^\star$ solution of the equation $\omega^2\tilde{x} - \partial V/\partial\tilde{x}|_{\tilde{y}=0} = f(t)E_0$ that is due to the competition between the Coulomb potential, the laser interaction and the Coriolis potential. At time t, the energy of the saddle point is denoted $\mathcal{Z}^\star(t) = \mathcal{Z}(\tilde{\mathbf{r}}^\star,t)$.

First, we consider a constant laser envelope with $f = 1$. Hamiltonian (3) is conserved in time, and its value is the Jacobi constant $\mathcal{K} = H(\tilde{\mathbf{r}},\tilde{\mathbf{p}})$. We apply the recollision picture in which the electron ionizes at time t_i and returns at time t_r such that $\tilde{\mathbf{r}}(t_i) \approx \tilde{\mathbf{r}}(t_r) \approx \mathbf{0}$ close to the core. Between the time t_i and t_r, the electron is in the continuum. Because of the Jacobi constant, $H(\tilde{\mathbf{r}}(t_i),\tilde{\mathbf{p}}(t_i)) = H(\tilde{\mathbf{r}}(t_r),\tilde{\mathbf{p}}(t_r))$ and the return energy of the electron is $|\tilde{\mathbf{p}}(t_r)|^2/2 \approx |\tilde{\mathbf{p}}(t_i)|^2/2$. Hence, the electron does not gain energy during its excursion in the continuum when it is driven by circularly polarized light even in the presence of the Coulomb potential, in agreement with Eq. (2).

When the laser envelope is taken into account, however, Hamiltonian (3) is no longer conserved and the energy of the recolliding electron can vary during its excursion. We consider $f(t)$ to be a 2-4-2 trapezoidal envelope. In Fig. 1, we show a typical recollision in CP fields seen in the rotating frame of an electron initialized with an energy $H(\tilde{\mathbf{r}},\tilde{\mathbf{p}},0) = -I_p$. The classically forbidden region (below the zero-velocity surface) is depicted in grey for $\tilde{y} = 0$. When the laser is turned off ($f = 0$), the electron motion is bounded. For hard-Coulomb potential, the maximum of the zero-velocity surface is $\mathcal{Z}^\star(0) \approx -(3/2)\omega^{2/3}$, i.e., the Coulomb barrier is decreased in the RF since this framework naturally includes the nonadiabatic effects. In a zeroth-order approximation, we consider two situations: If $I_p < (3/2)\omega^{2/3}$, as it is the case for the ionization potential used here, the electron is initially above the classical forbidden region, and a low laser intensity is sufficient to tear the electron off the core almost instantaneously, so $t_i \approx 0$. If $I_p > (3/2)\omega^{2/3}$, the electron is initially topologically bounded by the zero-velocity surface. The ionization is not instantaneous, so $t_i > 0$. For $t < t_i$, the time-dependent term $\tilde{x}E_0 f(t)$ in Hamiltonian (3) is very small, and therefore the energy is almost conserved $H(\tilde{\mathbf{r}},\tilde{\mathbf{p}},t) \approx -I_p$. For increasing time, the envelope increases and the energy of the saddle point decreases as $\mathcal{Z}^\star(t) \approx \mathcal{Z}^\star(0) - f(t)E_0\omega^{-2/3}$ for $f(t) \ll 1$. The ionization channel is opened when the energy of the

saddle point is the same as the ionization potential of the electron $\mathcal{Z}^\star(t_i) = -I_p$. Quantum mechanically, earlier ionization times can be accessible through tunneling. In any case, the electron ionizes close to the zero-velocity surface, and the electron initial kinetic energy E_i is small compared to the ponderomotive energy U_p.

After ionization, at time $t > t_i$, the electron is outside the bounded region and the time-dependent term $\tilde{x}E_0 f(t)$ in Hamiltonian (3) starts varying significantly compared to U_p. If t_i is relatively small $[f(t_i) \ll 1]$, the effective transverse potential vector $f(t_i)E_0/\omega$ is also small, and it can be compensated by the electron initial momentum, preventing the electron to drift away from the core after ionization in contrast to the case for which the ionization occurs when $f(t_i) \sim 1$. During its excursion, the electron spins around the zero-velocity surface. As we show later, the energy of the recolliding electron increases by a quantity of order U_p during the ramp-up. Therefore, the electron can populate high energy states. In particular, regions of phase space where periodic orbits can bring back this electron to the ionic core [18]. During the plateau, the electron dynamics evolves on a constant energy surface given by the Jacobi constant. At recollision time t_r, the electron is in the vicinity of the core, its energy is $\mathcal{E}_r = \mathcal{E}_i + \Delta\mathcal{E} \approx \Delta\mathcal{E}$, and a photon of frequency $\Omega = \mathcal{E}_r + I_p$ can be emitted.

The ionization time t_i is instrumental for the electron to come back. If t_i is too large, the initial velocity necessary to compensate the potential vector is too large to be reached by the electron after ionization, and it goes away without recolliding. Two parameters influence considerably the ionization time t_i: The ionization potential I_p and the laser frequency ω. Numerically, with the classical approach, we find that the electron potentially comes back to the core only if $I_p < I_c$, where I_c (eV) $\approx 50\ \omega$ (a.u.)$^{2/3}$ is the critical ionization potential. This expression is derived using a reduced model [19] (see Supplemental Material [20] for details). For $\omega = 0.0584$ a.u., the critical ionization potential is $I_c \approx 7.4$eV. If $I_p > I_c$, the ionization time t_i is too large and the electron drifts away from the core. We notice that $I_c/\mathcal{Z}(0) \approx -1.2$, which shows that the critical ionization potential is right below the saddle point energy. Conversely, for a given ionization potential, the laser frequency can be tuned for allowing recollisions with higher ionization potential in CP fields, as observed in Ref. [21]. Quantum mechanically, the wavepacket can tunnel ionize before their classical counterparts, and therefore increasing the critical ionization potential. Recollisions for CP are not always possible and more delicate than for low ellipticities.

In the RF with $\xi \neq 1$, the recollision picture is not so clear since the saddle moves in time even with fixed laser envelope. The scenario, however, works the same way. The electron initiated with a sufficiently small ionization potential ionizes early after that the laser field is turned on. After ionization, the initial momentum of the electron is relatively small and compensates the initial vector potential in Eq. (1), such that $\mathbf{p}(t_i) - \mathbf{A}(t_i) \approx \mathbf{0}$. The electron does not quickly drift away from the core. Then, the electron travels in the continuum. During its excursion in the continuum, the energy gained by the electron for slowly varying envelope is

$$\Delta\mathcal{E} \approx 2\mathrm{U}_p \left[f(t_r)^2 - f(t_i)^2\right] + 2\mathrm{U}_p(1-\xi^2)g(t_i,t_r), \quad (4)$$

where $g(t_i,t_r)$ is explicitely derived from the SFA [20]. Therefore, at high ellipticities, the electron mostly gains energy through the laser envelope [first term of the right hand-side of Eq. (4)]. In contrast, at low ellipticities, the electron mostly gains energy through the sub-cycle oscillations of the laser [second term of the right hand-side of Eq. (4)].

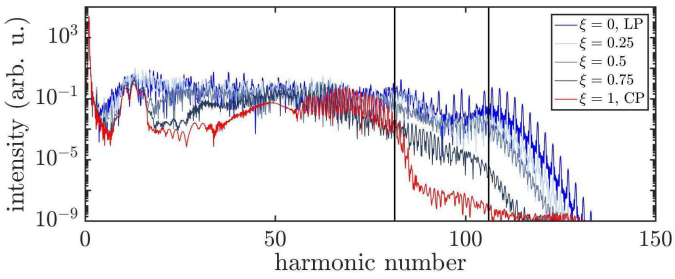

FIG. 2: HHG intensity spectrum for $\xi = 0$, 0.25, 0.5, 0.75 and 1. The vertical lines correspond to the radiated frequencies $2.3\mathrm{U}_p + I_p$ (left) and $3.17\mathrm{U}_p + I_p$ (right). (See text).

We use this classical recollision picture for the quantum calculations of HHG spectra. Figure 2 is the power intensity spectrum of the dipole acceleration [20]. The dipole acceleration is computed in the laboratory frame (LF) as a function of time $\mathbf{a}(t) = -\int \mathrm{d}^2\mathbf{r}\,|\Psi(\mathbf{r},t)|^2 \partial V(\mathbf{r})/\partial\mathbf{r}$ where $\Psi(\mathbf{r},t)$ is the wavefunction at time t solution of the two-dimensional time-dependent Schrödinger equation

$$i\frac{\partial}{\partial t}\Psi(\mathbf{r},t) = \left[-\frac{\Delta}{2} + V(\mathbf{r}) + \mathbf{r}\cdot\mathbf{E}(t)\right]\Psi(\mathbf{r},t). \quad (5)$$

The electric field in the LF is $\mathbf{E}(t) = E_0 f(t)[\hat{\mathbf{x}}\cos(\omega t) + \hat{\mathbf{y}}\xi\sin(\omega t)]$. We take the initial wavefunction in a superposition of states computed using imaginary time propagation and Gram-Schmidt orthonormalization such that $\Psi(\mathbf{r},0) = [\psi_0(\mathbf{r}) + \psi_1(\mathbf{r})]/\sqrt{2}$. The states $\psi_0(\mathbf{r})$ and $\psi_1(\mathbf{r})$ are the ground state and the first excited state of ionization potential $I_0 \approx 24.6$ eV and $I_p \approx 5.7$ eV, respectively (close to He). The superposition of state allows us to avoid the lack of HHG in CP fields due to the symmetries and the selection rules, and to avoid the emptiness of the ground state at the return of the electron originating from the excited state [22, 23]. In Fig. 2, we observe a cutoff at the 100th harmonic which corresponds to the electrons with return energy about $3.17\mathrm{U}_p$ for $\xi = 0$, 0.25 and 0.5. For larger ellipticities, the strength of the $80-160$th harmonics decreases significantly, and a second cutoff appears at the 80th harmonic corresponding to a return energy about $2.3\mathrm{U}_p$. We notice that this second cutoff is also observed at low ellipticity.

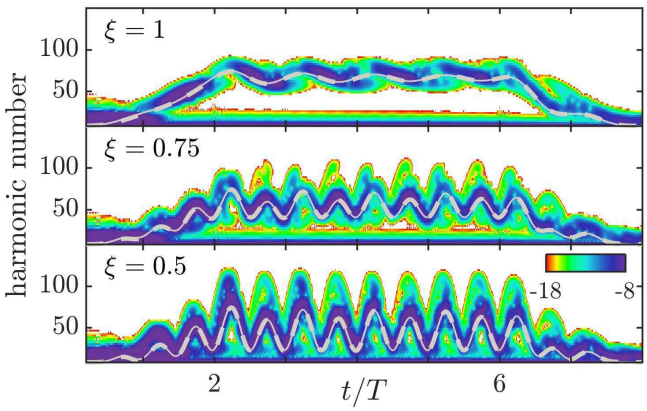

FIG. 3: Time-frequency analysis of the dipole acceleration $\mathbf{a}(t)$ at high ellipticities for a trapezoidal envelope 2-4-2. The solid and dashed curves overlap and correspond to the return energy and energy difference of the electron ionizing at time $t_i = 0$ and returning at time t_r in the SFA.

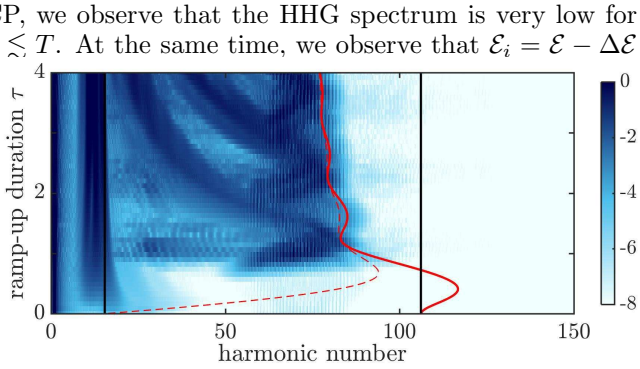

FIG. 4: HHG intensity spectrum (in arb. u.) as a function of the ramp-up duration τ/T in logarithmic scale for CP. The laser envelope is trapezoidal of ramp-up duration τ, plateau duration $6T - \tau$, and ramp-down duration $2T$. The dashed and solid red lines are the SFA prediction of the energy difference and return energy, respectively. All quantities are in a.u.

Figure 3 shows the time-frequency analysis of $\mathbf{a}(t)$ used for computing the HHG spectra of Fig. 2. We depict the return energy (solid grey curves) and the energy difference (dashed grey curves) of an electron ionizing at time $t_i = 0$ as a function of the return time computed in the SFA. We tested numerically that the depicted curves are robust with respect to the ionization time and no qualitative difference is observed on the dashed and solid curves for $t_i \lesssim 0.6T$. There is an excellent agreement between the grey curve and the maximum of the distribution of the time-frequency analysis. For $\xi = 0.5$, we observe a major contribution of the recollision channel described in this Letter and a minor contribution of the conventional recollision channel in which the electrons ionize and return during the plateau [24] with a maximum return energy around $3U_p$. For increasing ellipticity, the conventional recollision channel disappears [15] because of the large drift momentum of the electron at ionization [10]. Only the recollision channel described here persists. Also, the solid and dashed grey curves overlap almost completely for all return time and for all ellipticities, implying that the electron energy at ionization is very small.

The importance of the small electron energy at ionization (or small initial velocity) is demonstrated in Fig. 4 which shows the HHG spectrum as a function of the harmonic number and the ramp-up duration τ. The envelope is trapezoidal, the ramp-up is at $t \in [0, \tau]$, the plateau at $t \in [\tau, 6T]$ and the ramp-down at $t \in [6T, 8T]$. The solid and dashed red curves are the maximum return energy and the maximum energy difference in CP in the SFA, respectively, of the electron ionizing at time $t_i = 0$. For LP, the conventional recollision scenario is dominant. The spectrum follows the well known cutoff law $\Omega \approx 3.17U_p + I_p$ for all ramp-up duration τ. For CP, we observe that the HHG spectrum is very low for $\tau \lesssim T$. At the same time, we observe that $\mathcal{E}_i = \mathcal{E} - \Delta\mathcal{E}$ is large, and therefore the initial drift momentum of the electron pushes the electron away from the core without recolliding. The recollision channel described here is dominant, which depends drastically on the laser envelope, and we observe that the HHG cutoff oscillates as a function of the ramp-up duration for $\tau > T$. We observe a good agreement between the SFA prediction and the HHG cutoff.

In summary, we have demonstrated the conditions under which a large portion of electrons are both ionized and later return to their parent ion regardless the ellipticity of the laser field. For recollision, the electron needs to ionize early in during the ramp-up of the laser to benefit of the boost from the CP field and not to drift away from the core. For ionization early in the field, the ionization potential must be relatively small. We have shown that both the efficient ionization and recollisions are obtained for I_p (eV) $\lesssim 50\,\omega$ (a.u.)$^{2/3}$. During its excursion in the continuum, the electron gains energy dominantly from the envelope of the driving laser, and can exceed $2U_p$ allowing for a return energy $\mathcal{E}_r = \mathcal{E}_i + \Delta\mathcal{E}$ in excess of $2U_p$. Also, we observe a good agreement with the SFA if the the envelope is taken into account. This scenario is consistent with the enhanced experimental recollisions for high ellipticity in Ref. [25] for recollisions which occur in intensity range for which the ionization is over-the-barrier.

We thank Simon A. Berman and François Mauger for helpful discussions. The project leading to this research has received funding from the European Union's Horizon 2020 research and innovation program under the Marie Skłodowska-Curie grant agreement No. 734557. T.U. acknowledges funding from the NSF (Grant No. PHY1602823).

[1] K. J. Gaffney and H. N. Chapman, Science **316**, 1444 (2007).

[2] O. Smirnova, Y. Mairesse, S. Patchkovskii, N. Dudovich, D. Villeneuve, P. Corkum, and M. Y. Ivanov, Nature **460**, 972 (2009).

[3] M. Abu-Samha and L. B. Madsen, J. Phys. B: At. Mol. Opt. Phys. **51**, 135401 (2018).

[4] P. M. Paul, E. S. Toma, P. Breger, G. Mullot, F. Augé, P. Balcou, H. G. Muller, and P. Agostini, Science **292**, 1689 (2001).

[5] P. Salières and M. Lewenstein, Meas. Sci. Technol. **12**, 1818 (2001).

[6] S. Chatziathanasiou, S. Kahaly, E. Skantzakis, G. Sansone, R. Lopez-Martens, K. V. S Haessler, G. D. Tsakiris, D. Charalambidis, and P. Tzallas, Photonics **4**, 26 (2017).

[7] R. Bartels, S. Backus, E. Zeek, L. Misoguti, G. Vdovin, I. P. Christov, M. M. Murnane, and H. C. Kapteyn, Nature **406**, 164 (2000).

[8] P. G. Martínez, I. Babushkin, L. Bergé, S. Skupin, E. Cabrera-Granado, C. Köhler, U. Morgner, A. Husakou, and J. Herrmann, Phys.Rev. Lett. **114**, 183901 (2015).

[9] R. Boge, C. Cirelli, A. S. Landsman, S. Heuser, A. Ludwig, J. Maurer, M. Weger, L. Gallmann, and U. Keller, Phys. Rev. Lett. **111**, 103003 (2013).

[10] P. B. Corkum, Phys. Rev. Lett. **71**, 1994 (1993).

[11] K. J. Schafer, B. Yang, L. F. DiMauro, and K. C. Kulander, Phys. Rev. Lett. **70**, 1599 (1993).

[12] M. Lewenstein, P. Balcou, M. Y. Ivanov, A. L'Huillier, and P. B. Corkum, Phys. Rev. A **49**, 2117 (1994).

[13] M. V. Ammosov, N. B. Delone, and V. P. Krainov, Sov. Phys. JETP **64**, 1191 (1986).

[14] L. Arissian, C. Smeenk, F. Turner, C. Trallero, A. V. Sokolov, D. M. Villeneuve, A. Staudte, and P. B. Corkum, Phys. Rev. Lett. **105**, 113002 (2010).

[15] M. Möller, Y. Cheng, S. D. Khan, B. Zhao, K. Zhao, M. Chini, G. G. Paulus, and Z. Chang, Phys. Rev. A **86**, 011401(R) (2012).

[16] E. W. Larsen, S. Carlström, E. Lorek, C. M. Heyl, D. Paleček, K. J. Schafer, A. L'Huillier, D. Zigmantas, and J. Mauritsson, Sci. Rep. **111**, 263001 (2016).

[17] J. Javanainen, J. H. Eberly, and Q. Su, Phys. Rev. A **38**, 3430 (1988).

[18] A. Kamor, F. Mauger, C. Chandre, and T. Uzer, Phys. Rev. Lett. **110**, 253002 (2013).

[19] J. Dubois, S. A. Berman, C. Chandre, and T. Uzer, Phys. Rev. E **98**, 052219 (2018).

[20] See Supplemental Material for a derivation of the critical ionization potential, the return energy and difference energy in the SFA, and for details on the quantum calculations.

[21] X. Chen, Y. Wu, and J. Zhang, Phys. Rev. A **95**, 013402 (2017).

[22] F. Mauger, A. D. Bandrauk, A. Kamor, T. Uzer, and C. Chandre, J. Phys. B: At. Mol. Opt. Phys. **47**, 041001 (2014).

[23] P. M. Paul, T. O. Clatterbuck, C. Lynga, P. Colosimo, L. F. DiMauro, P. Agostini, and K. C. Kulander, Phys. Rev. Lett. **94**, 113906 (2005).

[24] J. Tate, T. Auguste, H. G. Muller, P. Salières, P. Agostini, and L. F. DiMauro, Phys. Rev. Lett. **98**, 013901 (2007).

[25] G. D. Gillen, M. A. Walker, and L. D. Van Woerkom, Phys. Rev. A **64**, 043413 (2001).